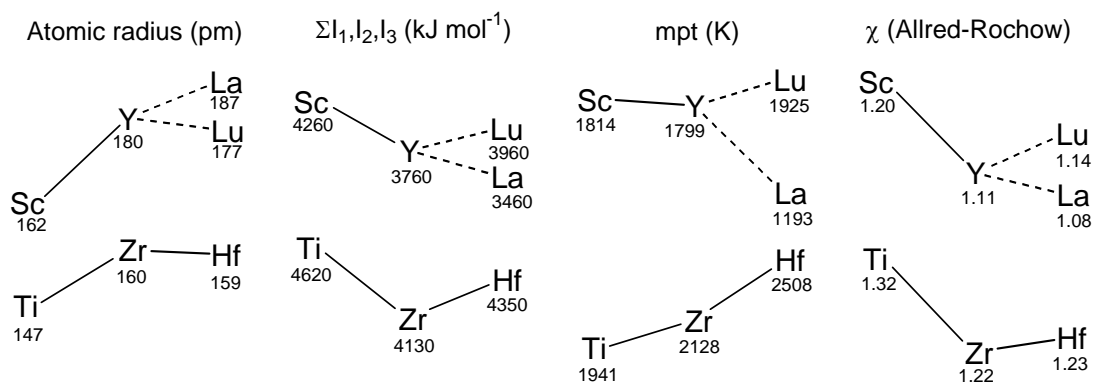
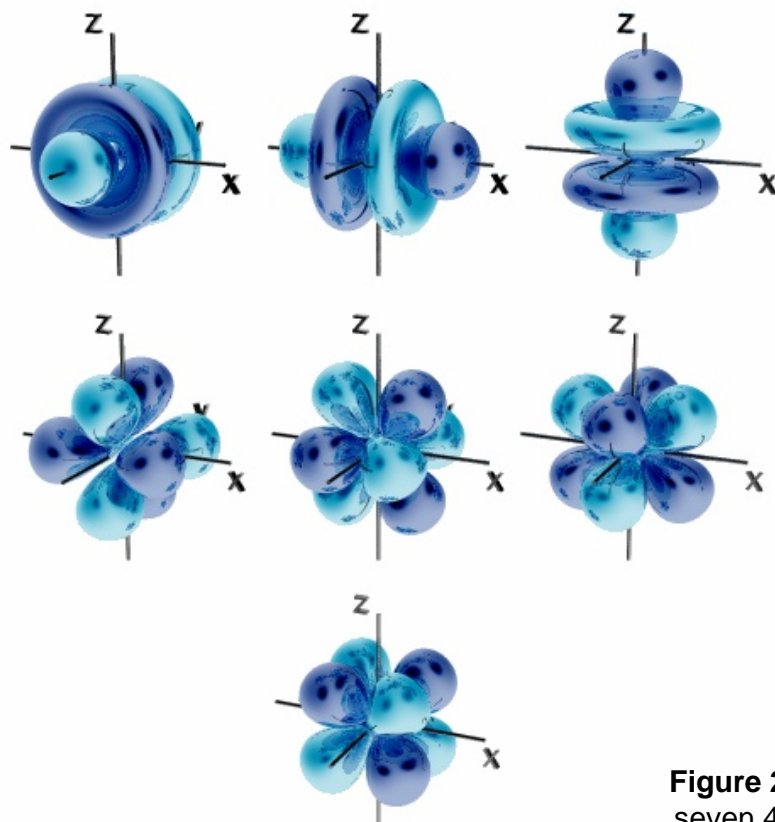


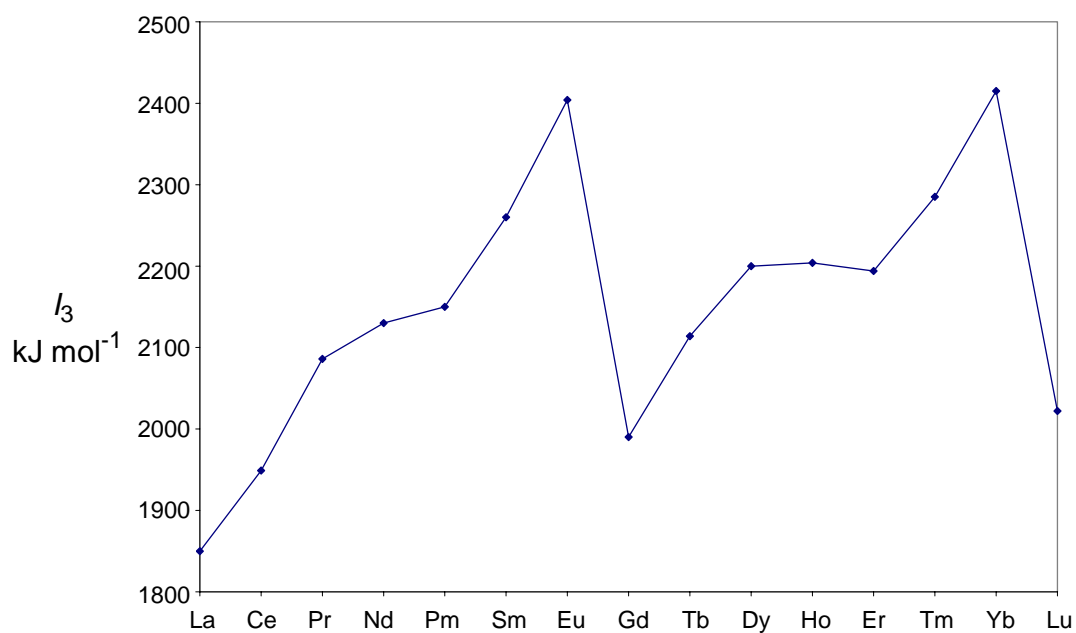
**Table 1.** Ground electronic configurations of the lanthanides

Element	Symbol	Atomic number	Electronic Configuration
Lanthanum	La	57	[Xe] 4f <sup>0</sup> 5d <sup>1</sup> 6s <sup>2</sup>
Cerium	Ce	58	[Xe] 4f <sup>1</sup> 5d <sup>1</sup> 6s <sup>2</sup>
Praseodymium	Pr	59	[Xe] 4f <sup>3</sup> 6s <sup>2</sup>
Neodymium	Nd	60	[Xe] 4f <sup>4</sup> 6s <sup>2</sup>
Promethium	Pm	61	[Xe] 4f <sup>5</sup> 6s <sup>2</sup>
Samarium	Sm	62	[Xe] 4f <sup>6</sup> 6s <sup>2</sup>
Europium	Eu	63	[Xe] 4f <sup>7</sup> 6s <sup>2</sup>
Gadolinium	Gd	64	[Xe] 4f <sup>7</sup> 5d <sup>1</sup> 6s <sup>2</sup>
Terbium	Tb	65	[Xe] 4f <sup>9</sup> 6s <sup>2</sup>
Dysprosium	Dy	66	[Xe] 4f <sup>10</sup> 6s <sup>2</sup>
Holmium	Ho	67	[Xe] 4f <sup>11</sup> 6s <sup>2</sup>
Erbium	Er	68	[Xe] 4f <sup>12</sup> 6s <sup>2</sup>
Thulium	Tm	69	[Xe] 4f <sup>13</sup> 6s <sup>2</sup>
Ytterbium	Yb	70	[Xe] 4f <sup>14</sup> 6s <sup>2</sup>
Lutetium	Lu	71	[Xe] 4f <sup>14</sup> 5d <sup>1</sup> 6s <sup>2</sup>

**Figure 1.** Periodic Trends, La vs. Lu


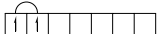


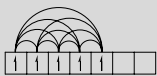
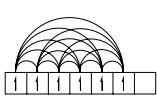
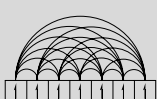


**Figure 2.** The shape of the seven 4f orbitals (cubic set)

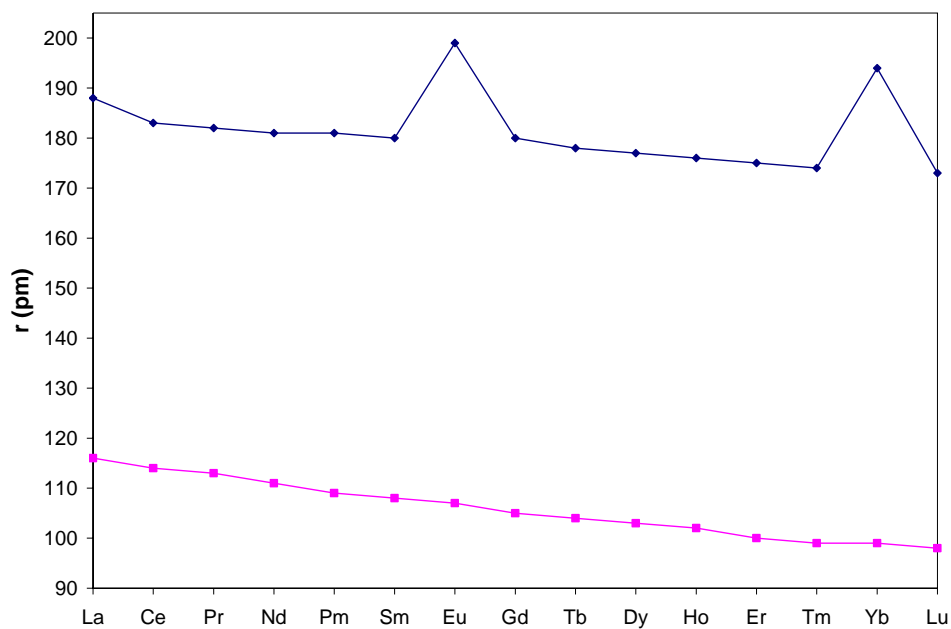


**Figure 3.** The variation of the third ionization energy ( $I_3$ ) of the lanthanides.

**Table 2.** Number of pairs of **parallel** spins for the  $f^n$  configurations.

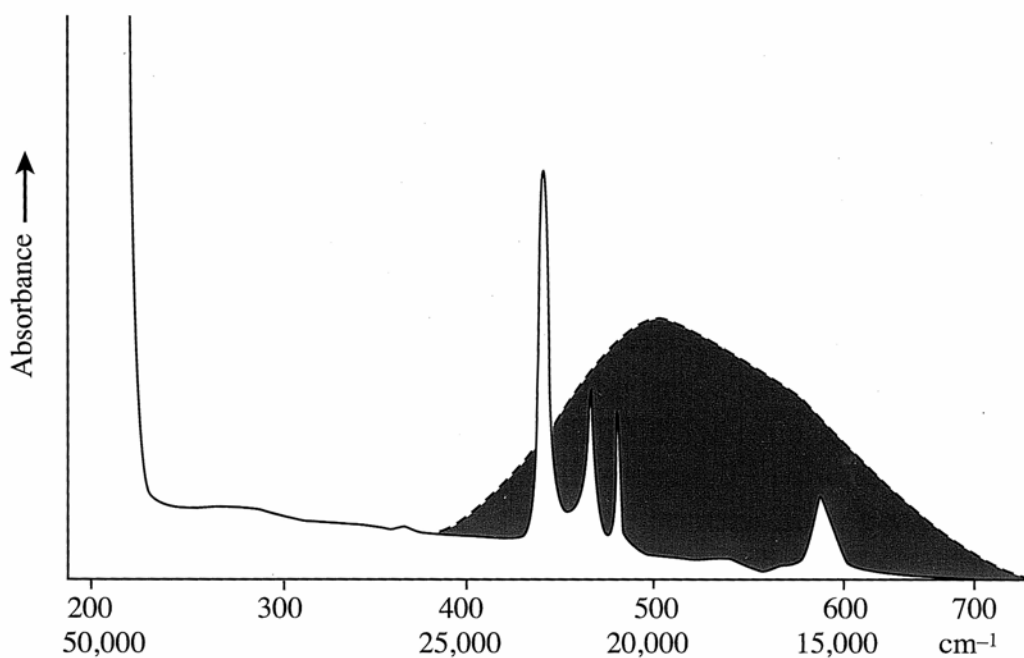
Configuration	$m$	$\delta m^*$	Configuration	$m$	$\delta m^*$	
$f^1$		0	0	$f^8$	21	0
$f^2$		1	1	$f^9$	22	1
$f^3$		3	2	$f^{10}$	24	2
$f^4$		6	3	$f^{11}$	27	3
$f^5$		10	4	$f^{12}$	31	4
$f^6$		15	5	$f^{13}$	36	5
$f^7$		21	6	$f^{14}$	42	6

\*  $\delta m$  refers to the number of pairs of parallel spins lost for the process  $f^n \rightarrow f^{n-1}$

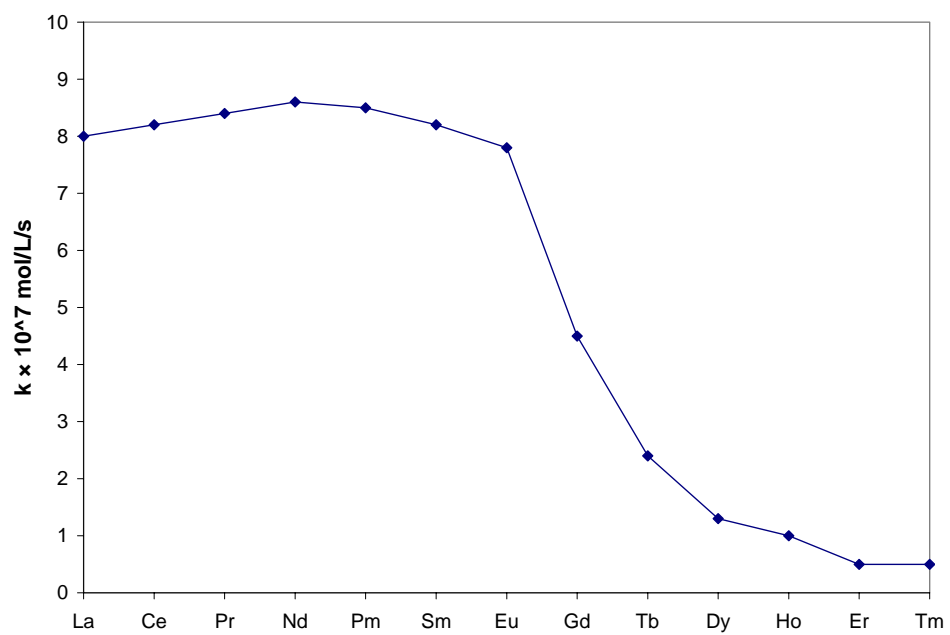
**Figure 4.** Variation of metal radius and +3 ionic radius for the lanthanide elements.

**Table 3.** Summary of the properties of Ln<sup>III</sup> ions.

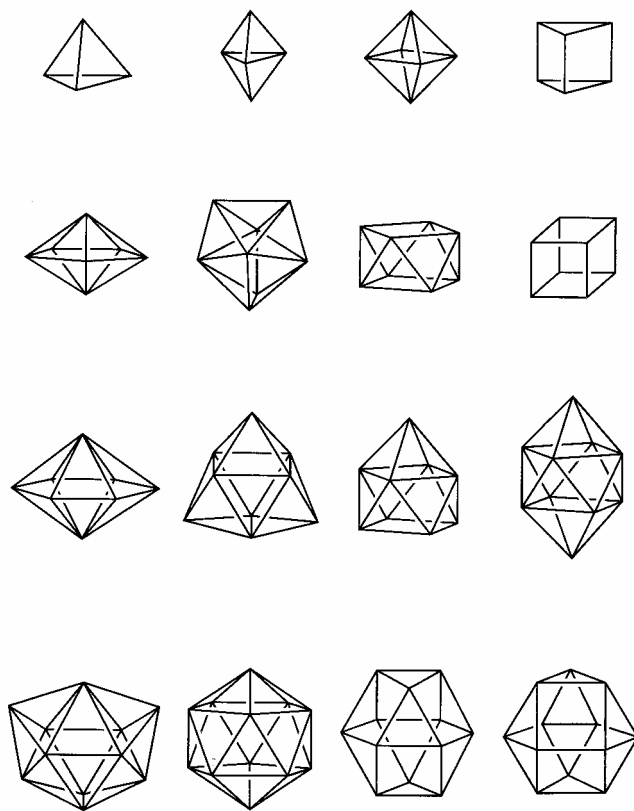
Ln <sup>3+</sup>	4f <sup>n</sup>	ground level	color	g [J(J+1)] <sup>1/2</sup>	Observed
La	0		colorless		0
Ce	1		colorless		2.3-2.5
Pr	2		green		3.4-3.6
Nd	3	<sup>4</sup> I <sub>9/2</sub>	lilac	3.62	3.5-3.6
Pm	4		pink		-
Sm	5		yellow		1.4-1.7
Eu	6		pale pink		3.3-3.5
Gd	7		colorless		7.9-8.0
Tb	8		pale pink		9.5-9.8
Dy	9		yellow		10.4-10.6
Ho	10		yellow		10.4-10.7
Er	11		rose-pink		9.4-9.6
Tm	12		pale green		7.1-7.5
Yb	13	<sup>2</sup> F <sub>7/2</sub>	colorless	4.54	4.3-4.9
Lu	14	<sup>1</sup> S <sub>0</sub>	colorless	0	0

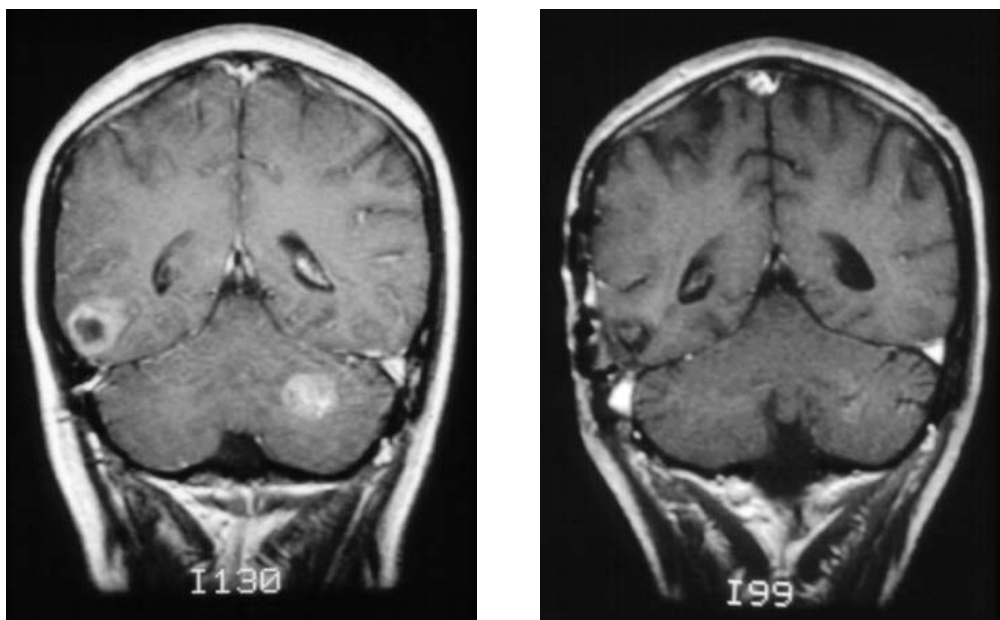


**Figure 5.** The electronic spectrum of Pr<sup>3+</sup> (solid line) and Ti<sup>3+</sup> (broken line). Like *d-d* transitions, *f-f* transitions are Laporte-forbidden and give weak absorptions.

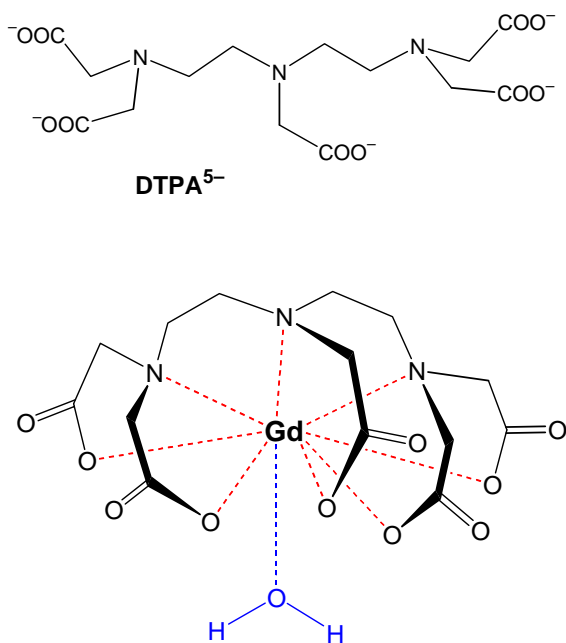


**Figure 6.** Rate constants for the formation of 1:1  $\text{Ln}^{3+}$ /oxalate complexes at 25° C.

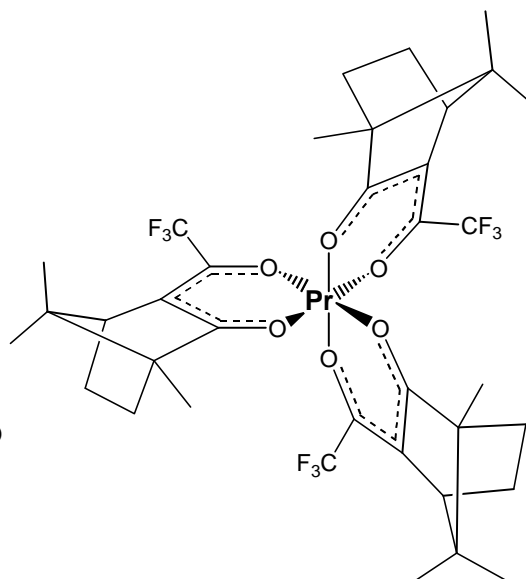




**Figure 7.** MRI scans with **Gd** enhancement before and after surgery and radiotherapy. The follow-up study shows minimal enhancement in the left cerebellar region, consistent with almost complete disappearance of the tumor mass.



**Figure 8.** The free  $\text{DTPA}^{5-}$  ligand, and its gadolinium complex. Note the additional coordination site available for water to bind to.



**Figure 9.** Chiral  $\text{Pr}^{3+}$  complex with three  $\beta$ -diketonate ligands.  $\text{Eu}^{3+}$  and  $\text{Pr}^{3+}$  are often used because their electronic relaxation times are very short, reducing line-broadening for the nucleus under study (usually  $^1\text{H}$ ).